

## Competing Templated and Self-Assembly in Supramolecular Polymers

Sara Jabbari-Farouji<sup>\*,†,‡,§</sup> and Paul van der Schoot<sup>†</sup>

<sup>†</sup>Theory of Polymer and Soft Matter group, Department of Applied Physics Eindhoven University of Technology, P.O. Box 513, 5600 MB Eindhoven, The Netherlands, and <sup>‡</sup>Dutch Polymer Institute, P.O. Box 902, 5600 AX Eindhoven, The Netherlands. <sup>§</sup>Present address: Le Laboratoire de Physique Laboratoire Théorique et Modèles Statistiques (LPTMS), Université Paris-Sud, 15 rue Georges Clémenceau, 91405 Orsay cedex, France

Received February 4, 2010; Revised Manuscript Received May 15, 2010

**ABSTRACT:** We put forward a coarse-grained model that describes the competition between the supramolecular polymerization of molecules and their binding to template molecules containing a fixed number of binding sites that are also present in the solution. Our model captures the salient features of the competition between this kind of self- and template-assisted assembly and demarcates conditions under which either is predominant. Template-assisted or “templated” assembly wins over self-assembly if the free energy gain of attaching of a monomer unit to a binding site is larger than that of binding it to a self-assembly. In order to find the optimal conditions for full coverage of the templates, we investigate the role of different control parameters such as stoichiometry and temperature on the binding efficiency. We also present a quantitative picture of the distribution of bound guest molecules along the templates for incompletely filled host molecules.

### 1. Introduction

Natural supramolecular structures such as liposomes, viruses, actin fibers, and amyloid fibrils have inspired scientists to exploit supramolecular self-assembly as a tool to design and construct desired molecular structures from synthetic molecular compounds.<sup>1,2</sup> Indeed, along these lines of effort, employing biomimetic self-assembly principles, complex structures as challenging as “smiley faces”<sup>3</sup> and interlocking rings (Borromean rings)<sup>4</sup> have been constructed from DNA. The most common (and much simpler) type of supramolecular assembly is that of the so-called equilibrium polymer (EP), in which all the monomeric molecular building blocks are able to bond reversibly with each other and form quasi-linear self-assemblies of varying length.<sup>5–8</sup> The growth of these assemblies can take place either in the form of isodesmic self-assembly (“free association”) or of nucleated assembly in which an energy barrier must be overcome in one or a few steps in the cascade of addition reactions. The main feature of EPs is their exponential size distribution, which makes them inherently very polydisperse. The average molecular weight can be influenced by varying the temperature and concentration of the monomers or by adding so-called chain stoppers. The polydisperse nature of self-assembled polymers cannot easily be altered as it results directly from the law of mass action.

A way to overcome this for some applications undesirable feature is to use *host* templates consisting of a definite number of binding sites to which *guest* monomers can be bound, leading (in principle) to self-assembled but monodisperse supramolecular strands. Obviously, this strategy works only if the affinity of the guest molecules for the binding sites is larger than that for themselves to polymerize. In Nature templates with specific binding sites can be found that efficiently form assemblies with predefined size or sequence. For instance, in linear viruses such as the cylindrical tobacco mosaic virus (TMV) single-stranded

RNA acts as a tape-measure molecule for the directed assembly of the coat proteins of the virus.<sup>9–11</sup> A similar mechanism has been suggested for the self-assembly of coat proteins of spherical viruses.<sup>11,12</sup> Interestingly, in tailed bacteriophages the tail length seems to be regulated by a ruler or tape-measure protein, around which the tail tube monomers polymerize.<sup>13</sup> As another example one can mention the binding of RecA proteins to double-stranded DNA.<sup>14</sup>

All of this has inspired researchers to exploit template-assisted or “templated” polymerization as a tool to control the size and sequence of synthetic supramolecular polymers via a bottom-up approach, where the shape of molecule is specifically designed.<sup>15–19</sup> Probably one of the simplest systems based on this kind of bottom-up method are given by double-stranded homopolymeric DNA hybrids constructed from naphthalene-type chromophores, acting as guest molecules, hydrogen bonded to single strands of oligothymine that act as the host template molecules.<sup>18,19</sup> Here, in addition to the hydrogen bonds formed between guest and host molecules,  $\pi$ – $\pi$  stacking interactions between neighboring bound monomers enhance the templated assembly in this kind of structure, in fact mimicking similar effects in actual double-stranded DNA.

The binding efficiency of the guest molecules may be quantified by the average fraction of filled binding sites of a template, i.e., the so-called bound fraction. Experimentally, the bound fraction can be determined spectroscopically and its dependence probed as a function of the overall concentration, the temperature, and the relative ratio of number density of guests to host binding sites (the so-called stoichiometric ratio). Because chromophore binding via hydrogen bonding is exothermic, i.e., enthalpy-driven, the bound fraction increases upon decreasing the temperature and saturates for sufficiently low temperatures when full coverage of the templates is achieved.<sup>18,19</sup> Note that with increased coverage the conformation of the templates plausibly changes from a disordered coil to a rodlike or helical configuration, in particular if the template is single-stranded DNA.

\*To whom correspondence should be addressed. E-mail: sara.jabbari@u-psud.fr.

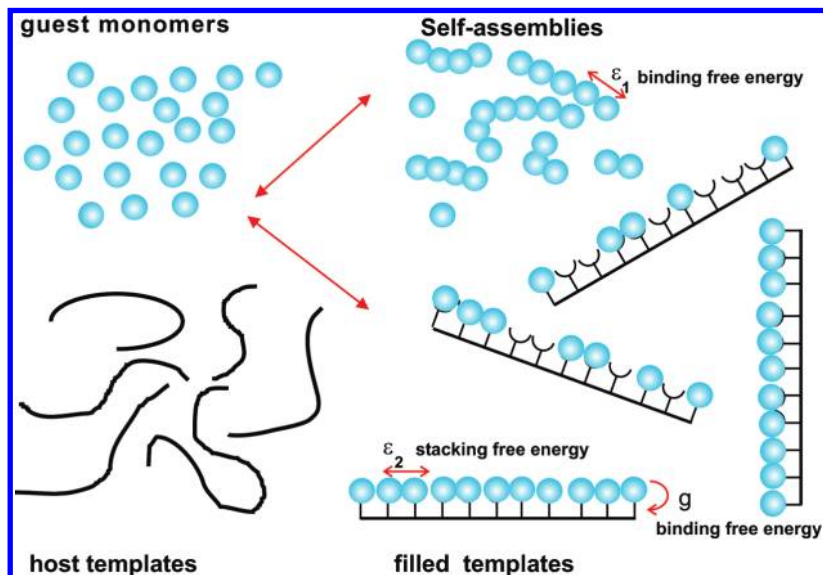


**Figure 1.** Schematic representation of our model system, consisting of guest molecules (filled circles) and template molecules (drawn lines) with  $q$  binding sites on them. The guest molecules can reversibly polymerize, if the binding free energy,  $\epsilon_1$ , is negative, or bind to binding sites on the templates, if the binding free energy,  $g$ , is negative. If two guests bind on neighboring sites on the template, this liberates a stacking free energy,  $\epsilon_2$ .

Recent experiments indicate that for guest concentrations higher than some value, or temperatures that are sufficiently low, linear self-assembly may also set in, induced by the aforementioned stacking interactions.<sup>19</sup> This suggests that there must, if only in principle, always be a competition between templated and self-assembly. In fact, under some experimental conditions, linear self-assembly could plausibly become the predominant mode of self-organization. Motivated by the mentioned experimental work, we investigate theoretically in this paper both types of assembly and argue that the issue is of considerable interest. First, understanding the behavior of competing self-assembling systems is of fundamental theoretical significance that has received little attention in the literature (see, however, refs 20 and 21). Second, insights gained may be of use in designing and/or optimizing template-assisted assembly systems, in particular how to tune the intermolecular interactions and concentrations of species involved in the experiments.

Our theoretical approach is a coarse-grained one that ignores the chemical details of the molecular structures and only considers the most important interactions governing the assembly included in the model as adjustable free energy parameters (see Figure 1). The relevant free energy for the self-assembly is a stacking or binding free energy of monomers in a linear supramolecular polymer,  $\epsilon_1$ . For the templated-assembly route, we have a net binding free energy of monomers to the host templates,  $g$ , which includes the free energy for the change of the conformational state of a monomer from that in free solution to that bound on the template, and a stacking free energy of two adjacently bound monomers  $\epsilon_2$ .

From our calculations, we conclude that the relevant quantity governing the predominance of either type of assembly is the free energy difference,  $\Delta F$ , between a monomer attached to a binding site adjacent to an occupied site on a template and that of a monomer binding to one end of a preexisting self-assembly, so  $\Delta F = g + \epsilon_2 - \epsilon_1$ . Predominance of templated assembly requires that this quantity is negative. Interestingly, in such a templated-assembly predominant case, no self-polymerization occurs until all the templates are filled. This implies that with increasing guest monomer concentration, the monomers favor occupying the template sites rather than self-assembling until they almost completely fill the templates, and it is only after this happens that linear self-assemblies are formed in coexistence with the templated assemblies.

In the opposite case where the free energy gain from binding of a monomer to a self-assembly is larger than that of binding to a vacant template site adjacent to a bound site and  $\Delta F$  is positive, self-assembly is dominant. Strikingly, in this case the templates are only partially filled even for highest concentrations of guest monomers. Even a slightly positive  $\Delta F$  is sufficient to impair the templated assembly and for the case of  $\Delta F = 0$ ; at most only half of the templates binding sites can get filled. This asymmetry in the assembly behavior for positive and negative values of the free energy  $\Delta F$  originates from the fact that the number of template molecules, and hence the number of binding sites is limited, while effectively there is no limitation on the length or the number of the self-assemblies.

The remainder of this paper is organized as follows. In section 2, we first describe the theoretical model, which is a combination of theory of linear self-assembly and Ising-like model for templated assembly. In section 3, we present generic state diagrams and discuss in detail the regimes where templated assembly and self-assembly predominate and where neither has the upper hand. We find that in the templated assembly dominated regime, no self-polymerization occurs before all the templates are by and large filled. Hence, under experimental conditions where full binding is not achieved, the system behaves essentially as in the case of exclusively templated assembly, that is, with monomers that have no tendency to self-assembly. Therefore, in section 4, we focus on the case of exclusively templated assembly and explore in considerable detail the effect of the size of template, cooperativity, and the stoichiometric ratio on the bound fraction of guest molecules.

In section 5, we investigate the issue of the distribution of guests over the templates for incompletely filled templates. We show that mapping the templated assembly problem onto an Ising model enables us to calculate the relevant probability distribution functions and obtain a clear picture of the monomer distribution on templates of varying length. To make a direct link to experiments in which the temperature dependence of the bound fraction are measured, we devote the section 6 to calculating the bound fraction and fraction of monomers in self-assemblies as a function of the temperature. Finally, we end our paper with section 7 where we summarize our main findings and results and provide a discussion of our work in relation to the existing literature and recent experimental results.

## 2. Theory

In this section we present an equilibrium theory for assembly in a two-component system consisting of guest monomers and host template molecules, in a solvent the properties of which are included effectively in the model parameters. The monomers can either bind reversibly to themselves to form quasi-linear polymer-like self-assembling structures of an arbitrary degree of polymerization  $N$  or bind (also reversibly) to available binding sites on the host templates (see Figure 1). In our model we ignore the details of molecular structure of the various components, and the host molecules are considered as quasi-one-dimensional objects with  $q$  binding sites onto which the monomers can bind. The relevant interactions driving the assembly both on and off the templates are parametrized by phenomenological, temperature-dependent effective free energies and understood to include solvophobic interactions as well as, e.g., electrostatic, van der Waals, hydrogen bonding,  $\pi$ - $\pi$  interactions, and so on.

Let  $\varepsilon_1 < 0$  denote the free energy of the bonded interaction between two monomers in a self-assembly,  $\varepsilon_n > 0$  a nucleation free energy originating from the change of monomers conformations due to binding,  $g < 0$  the free energy of binding of a monomer to a binding site on the template, and  $\varepsilon_2 < 0$  the stacking free energy between two adjacent monomers bound on the same template (see Figure 1). In our model description,  $g$ ,  $\varepsilon_1$ ,  $\varepsilon_2$ , and  $\varepsilon_n$  are free parameters made dimensionless by scaling them to the thermal energy  $k_B T$ , with  $k_B$  Boltzmann's constant and  $T$  the absolute temperature. As already alluded to in the Introduction, these free energies can originate from different types of interactions. For example, in the pertinent system of Janssen et al.,<sup>18</sup> involving naphthalene-type guest monomers and homopolymeric ssDNA, the binding free energy  $g$  results from three hydrogen bonds between the monomer molecule and a single binding site, and the stacking free energies  $\varepsilon_1$  and  $\varepsilon_2$  are mainly due to  $\pi$ - $\pi$  interactions between two adjacent bound guest molecules. The stacking free energy  $\varepsilon_2$  of two neighboring monomers bound to a template can be different from that in the form of self-assemblies  $\varepsilon_1$ : the template backbone plausibly influences the relative distance of two adjacent monomers through its chemical structure or lost configurational degrees of freedom that influence the net binding free energy. The nucleation free energy  $\varepsilon_n$  originates from loss of conformational entropy due to self-assembly of free monomers.

The (dimensionless) grand potential  $\Omega$  of our system consists of the sum of the contributions from the free monomers and the self-assembled polymers and that of the empty and bound templates, and which are functions of the chemical potentials of the monomers and host templates,  $\mu_g$  and  $\mu_h$ . These are fixed by the concentration of guest molecules,  $\phi_g$ , and host templates,  $\phi_h$ , present in the solution. Presuming no additional interactions between the different components than the ones already mentioned, we presume the solution to be dilute, in which case the grand potential can be written as

$$\frac{\Omega}{V} = \sum_{N=1}^{\infty} \rho_g(N) \left[ \ln \left( \frac{\rho_g(N)v}{e} \right) - \ln Z_{EP}(N) - \mu_g N \right] + \sum_{n=0}^q \rho_h(n) \left[ \ln \left( \frac{\rho_h(n)v}{e} \right) - \ln Z_q(n, g, \varepsilon_2) - \mu_h - n\mu_g \right] \quad (1)$$

Here,  $v$  denotes the so-called interaction volume that we take as the volume of solvent molecules,  $V$  the volume of the system,  $\rho_g(N)$  the number density of chains of degree of polymerization  $N$ , and  $\rho_h(n)$  the number density of templates with  $n$  monomers bound to them.  $Z_{EP}(N)$  and  $Z_q(n, g, \varepsilon_2)$  are partition functions of a self-assembled polymer with  $N$  monomers and of a template with

$n$  occupied binding sites, respectively. The partition functions count the number of configurational states of the chains and weigh these according to their Boltzmann weight.

From established polymer theory, the partition function of a polymer with  $N$  degree of polymerization has the generic form which is a product of several factors, i.e., the single particle partition function, the partition function counting possible arrangements of monomers in the chain, and the Boltzmann weight taking into account the bare free energy of  $N$  bonds.<sup>2</sup> This partition function,  $Z_{EP}(N)$ , can be renormalized and written in terms of effective free energies and becomes equal to  $\exp(\varepsilon_n)$  for a single free monomer and to  $\exp((N-1)\varepsilon_1)$  for an  $N$ -mer with  $N > 1$ . The partition function of a template with  $n$  occupied sites is

$$Z_q(n, g, \varepsilon_2) = \sum_{\{n_i\}} \delta_{\sum_{i=1}^q n_i, n} \exp[-G_1(\{n_i\})] \quad (2)$$

in which  $\delta_{ij}$  is the Kronecker delta and each configuration of a template is represented by a set of occupation numbers  $n_i = 0, 1$  for  $i = 1, 2, \dots, q$ . The occupation number of each site on the template is zero if no guest monomer is bound and one if a guest monomer is bound to it. Within our model, the free energy change associated with a specific configuration  $\{n_i\}$  of bound guests on a template with respect to reference state of empty templates reads

$$G_1(\{n_i\}) = \varepsilon_2 \sum_{i=1}^{q-1} n_i n_{i+1} + g \sum_{i=1}^q n_i \quad (3)$$

again in units of thermal energy. Here,  $\varepsilon_2$  and  $g$  include the contribution from free energy change configurational statistics of the guest and the backbone template due to binding. This allows us to calculate  $Z_q(n, g, \varepsilon_2)$  explicitly. We do this below.

The equilibrium size distributions  $\rho_g(N)$  and  $\rho_h(n)$  optimize the grand potential eq 1, and hence we set  $\delta\Omega_{tot}/\delta\rho_g(N) = 0$  to obtain

$$\begin{aligned} \rho_g(1) &= v^{-1} \exp(\mu_g) \exp(\varepsilon_n), \quad \rho_g(N > 1) \\ &= v^{-1} \exp(\mu_g N) \exp(-\varepsilon_1(N-1)) \end{aligned} \quad (4)$$

showing that the size distribution of linear self-assemblies has an exponential size dependence, implying polydisperse supramolecular polymers. Note that  $\exp(\mu_g)$  is related to the number density of unbound free monomers in the solution, itself linked to the overall concentration of guest molecules  $\phi_g$ . With the distribution of self-assemblies number density known, the fraction of guest molecules in self-assemblies can be calculated from  $\lambda = \sum_{N=2}^{\infty} N \rho_g(N) v / \phi_g$ .

Turning now to the templated assemblies, we obtain their distribution by setting  $\delta\Omega_{tot}/\delta\rho_h(n) = 0$

$$\rho_h(n) = v^{-1} \exp(\mu_h) Z_q(n, g, \varepsilon_2) \exp(n\mu_g) \quad (5)$$

This distribution function can be extracted from experimental data for large template sizes once we know the bound fraction, as we shall discuss in section 5. Indeed, the quantity of interest amenable to the experimental observation is the mean fraction of occupied sites  $\langle \theta \rangle = \langle n \rangle / q$  with  $\langle n \rangle = \sum_{n=1}^q n \rho_h(n)$ . The bound fraction  $\langle \theta \rangle$  can be calculated from grand partition function  $Q(\mu, g, \varepsilon_2) = \sum_{n=0}^q Z_q(n, g, \varepsilon_2) \exp(n\mu_g) = \sum_{n=0}^q \rho_h(n)$ , which is Laplace transform of the canonical partition function.

To calculate the grand partition function  $Q$ , which counts all the possible configurations of the templates with different degrees of occupancy, we for simplicity map it to the Ising model with the transformation  $n_i = 1/2(S_i + 1)$ , with  $S_i = \pm 1$  the spin states of the sites. Next, we apply the standard transfer-matrix method<sup>22</sup> to

obtain it explicitly. The grand partition function in this representation has the form  $Q = \sum_{S_i=\pm 1} \exp(-G(\{S_i\}))$ , in which

$$G(\{S_i\}) = -J \sum_{i=1}^{q-1} S_i S_{i+1} - H \sum_{i=1}^q S_i + \frac{\varepsilon_2}{4}(1 + S_1 + S_q) + E_0 \quad (6)$$

with  $J \equiv -\varepsilon_2/4$ ,  $H \equiv (-\varepsilon_2 - g + \mu_g)/2$ , and  $E_0 \equiv q(\varepsilon_2/2 + g - \mu_g)/2$ . Knowing the relation of our model parameters to the coupling constant  $J$  and magnetic field  $H$  in the Ising model, it is now straightforward to calculate the grand partition function in terms of the eigenvalues,  $\lambda_{\pm}$ , of the transfer matrix.

The resulting partition function takes the form  $Q(s, \sigma, q) = x\lambda_+^q + y\lambda_-^q$ , in terms of the eigenvalues  $\lambda_{\pm} = 1/2[1 + s \pm ((1-s)^2 + 4\sigma s)^{1/2}]/(\sigma s^2)^{1/4}$  with  $\sigma \equiv \exp(\varepsilon_2)$  and  $s \equiv \exp(-\varepsilon_2 - g + \mu_g)$ . Note that here we have introduced a similar terminology as in the Zimm–Bragg model of helix–coil transition in biopolymers.<sup>23</sup> The quantity  $s$  describes the statistical weight for occurrence of two adjacent bound sites on the templates, and  $\sigma$  is a measure of cooperativity in the assembly; a small  $\sigma$  implies a large negative value of  $\varepsilon_2$ , leading to a more cooperative assembly, as we shall discuss in more detail in the following sections. The quantities  $x$  and  $y$  denote factors that depend on the boundary conditions that we impose on the state of first and last site of the templates. We shall not impose any boundary condition; i.e., both the first and last binding site on each template can be either empty or occupied. This gives  $x = (s\sigma + 1 - (s^2\sigma)^{1/4}\lambda_-)/(s\sigma)^{1/2}(\lambda_+ - \lambda_-)$  and  $y = (s\sigma + 1 - (s^2\sigma)^{1/4}\lambda_+)/(s\sigma)^{1/2}(\lambda_- - \lambda_+)$ .

The mean bound fraction  $\langle \theta \rangle$  of sites can be expressed in terms of mean spin state  $\langle S \rangle$  through  $\langle n \rangle = 1/2(1 + \langle S \rangle)$  and calculated from logarithmic derivative of grand potential<sup>22</sup>

$$\langle \theta \rangle(s, \sigma, q) = \frac{1}{2} + \frac{1}{q} \frac{\partial \ln Q}{\partial \ln s} \quad (7)$$

In general,  $\langle \theta \rangle$  is a function of binding and stacking free energies as well as the length of template. The dependence of  $\langle \theta \rangle$  on the total molar fraction of guests  $\phi_g$  and binding sites of the host templates  $\phi_h$  can be made explicit by invoking the conservation of total number of guest monomers. In total, we have two mass conservation constraints, one for each of the guest and host molecules.

The overall molar fraction of guest monomers is equal to the sum of the molar fraction of free guest monomers, monomers bound in self-assemblies, and monomers bound on the template. The total molar fraction of binding sites is the sum of all the possible configuration of templates with 0, 1, ...,  $q$  occupied binding sites times the number of binding sites per template,  $q$ . So, our two constraints, i.e., equations of mass conservation, are

$$\sum_{N=1}^{\infty} N \rho_g(N) v + \langle \theta \rangle \phi_h = \phi_g \quad (8)$$

$$q \sum_{n=0}^q \rho_h(n) v = \phi_h \quad (9)$$

It turns out useful to reexpress eq 8 in terms of two mass action variables, being  $X_g \equiv \phi_g \exp(-\varepsilon_1)$  and  $X_h \equiv \phi_h \exp(-\varepsilon_2 - g)$  characterizing the strength of the driving force for self- and templated assembly. Indeed,  $X_g$  and  $X_h$  are proportional to the a priori probabilities of binding of a free monomer either to another one or to a free binding site on a template.

Taking advantage of eq 4 and performing the sum over  $N$  and expressing everything in terms of mass action variables gives the following form for the mass conservation equation, eq 8

$$s(e^{\varepsilon_n} - 1) + \frac{s}{(1 - se^{\Delta F})^2} + X_h \langle \theta \rangle(s, \sigma, q) - X_g e^{-\Delta F} = 0 \quad (10)$$

where  $\Delta F \equiv \varepsilon_2 + g - \varepsilon_1$  is an aforementioned free energy that describes the free energy difference of attaching a guest to a template next to an occupied site and that of attaching one to free end of a linear supramolecular polymer. As we shall see in the next section,  $\Delta F$  is a crucial parameter, and the cases  $\Delta F \geq 0$  and  $\Delta F < 0$  give rise to different types of predominant assembly. Equations 7 and 10 can be solved to eliminate the parameter  $s$ , hence the chemical potential from the equations to determine the bound fraction and number-averaged size of self-assemblies.

To compare the contribution of monomers in the form of self-assemblies with that of templated assembly, we need to know the fraction of self-assemblies. This quantity can also be expressed in terms of mass action variable  $X_g$  and  $\Delta F$ , giving

$$\lambda(s, X_g, \Delta F) = \frac{\sum_{N=2}^{\infty} N \rho(N)}{\phi_g} = \frac{se^{\Delta F}}{X_g} \left( \frac{1}{(1 - se^{\Delta F})^2} - 1 \right) \quad (11)$$

So, solving eq 11 with the constraint eq 10 provides us with the fraction of guest molecules in self-assemblies.

Having all the tools in hand, we analyze the model in the next section to obtain the general behavior of system as a function of the mass action variables and of the free energy  $\Delta F$ . As a nonzero nucleation free energy  $\varepsilon_n$  does not change the predictions of our model qualitatively, and to reduce the number of parameters, we set  $\varepsilon_n = 0$  from now on in the remainder of the paper.

### 3. Predominant Assemblies and State Diagram

In this section, we focus on a general description of what states of assembly predominate, as one varies the strength of the various mass action variables. Both the fraction of self-polymerized material and the bound fraction (of guest molecules on the templates) are in principle functions of the concentrations  $\phi_h$  and  $\phi_g$  and of the binding free energies  $\varepsilon_1$ ,  $\varepsilon_2$ , and  $g$ . However, because of the constraint of mass conservation, eq 10, we can rearrange the variables and express the desired quantities as a function of only four independent variables, being two dimensionless concentrations,  $X_h$  and  $X_g$ , and two free energies,  $\Delta F$  and  $\varepsilon_2$ , where it turns out expedient to express the latter in terms a Boltzmann weight  $\sigma \equiv \exp(\varepsilon_2)$ . As we shall see, for some experimental situations, it is convenient to convert this set into one consisting of a dimensionless concentration  $X_h$ , a stoichiometric ratio  $\eta = \phi_g/\phi_h$ , and the free energy parameters  $\sigma$  and  $\Delta F$ .

As we already mentioned in the previous section,  $\Delta F$  plays a crucial role in determining the state of assembly of guest molecules. It describes the difference in free energy gain of binding of a monomer next to an already bound site on a free template site and that of attaching a free monomer to a free end of a self-polymer. Therefore, depending on  $\Delta F$  being positive or negative, we expect that either self-assembly or templated assembly will be predominant, in accordance with basic thermodynamic principles.

The crossover from no to full assembly occurs gradually with increasing guest and host mass action variables. The fraction of self-polymerized material is characterized by the quantity  $\lambda$ , and the fraction of polymerized material bound to the templates is quantified by the bound fraction of sites  $\langle \theta \rangle$ , the values of which raise gradually from 0 to 1 with increasing of mass action variables. For definiteness, we define  $\lambda = 1/2$  as the transition

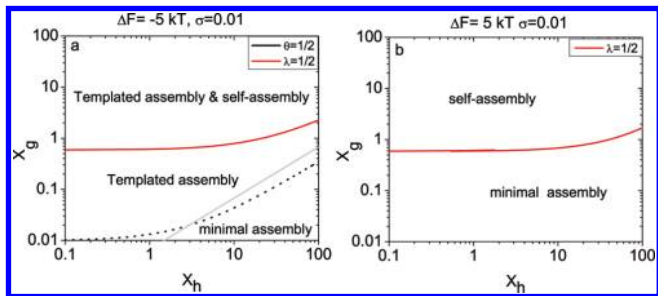


**Figure 2.** State diagram of self- and template-assembled polymers as a function of the mass action variables  $X_g$  and  $X_h$  driving the self- and templated-assembly for (a)  $\Delta F < 0$  and (b)  $\Delta F \geq 0$ , for a finite length of template  $q = 10$ . The light gray line indicates equal number of guest molecules and host binding sites, i.e.,  $\phi_g/\phi_h = 1$ .

point of self-assembly and  $\langle \theta \rangle = 1/2$  as the transition point of templated assembly. Within these definitions, a templated-assembly dominant regime is determined by  $\langle \theta \rangle > 1/2$  and  $\lambda < 1/2$ , a self-assembly dominant regime is where  $\lambda > 1/2$  and  $\langle \theta \rangle < 1/2$ , and we have significant coexistence of templated and self-assembly if both  $\lambda > 1/2$  and  $\langle \theta \rangle > 1/2$ . If  $\lambda$  and  $\langle \theta \rangle$  are both less than  $1/2$ , and the guest molecules are present mainly in the form of free monomers with no type of assembly being predominant (so-called minimal assembly). We define the boundaries between the different regimes by the equalities  $\lambda = 1/2$  and  $\langle \theta \rangle = 1/2$ . The equations describing these boundaries can be obtained from eqs 7, 10, and 11. In accordance with expectation, we find for the two main regimes: (i) the templated-assembly dominant regime for  $\Delta F < 0$  and (ii) the self-assembly dominant regime for  $\Delta F \geq 0$ .

Figure 2 shows two state diagrams for both these main cases. The lines indicate the crossovers  $\lambda = 1/2$  and  $\langle \theta \rangle = 1/2$  in the  $X_h$ - $X_g$  plane, as clarified in the caption. In the templated dominant regime, where  $\Delta F < 0$ , we observe that upon increasing the guest concentration,  $X_g$ , at fixed host concentration,  $X_h$ , first at least half of the templates are filled. In fact, as we shall show below, it is only after virtually all the templates are filled that the excess of free monomers in the solution can take mass action to induce self-assembly and  $\lambda$  reaches the value of one-half. Also, indicated in Figure 2a by a gray line are conditions of “perfect stoichiometry” where  $\phi_g = \phi_h$ , that is, the minimum amount of guest molecules needed to be present in the solution to fill all the template sites.

In Figure 2a we recognize two regimes for the crossovers  $\langle \theta \rangle = 1/2$  and  $\lambda = 1/2$ : a horizontal part with slope zero and a part with slope unity. To understand this, one should keep in mind that the amount of guest concentration needed to fill half of the binding sites is equal to  $\phi_g = \phi_h/2$ , which in terms of mass action variables becomes  $X_{g1} = X_h e^{\Delta F}/2$ . From eq 10, we then find that the contribution of self-polymerization and free monomers to guest mass action in such a situation (where  $s \approx 1$  is roughly equal to  $X_{g2} = e^{\Delta F}(1 - e^{\Delta F})^{-2}$ ). Therefore, if the number of monomers in the form of self-polymerization and free ones is predominant over the number of monomers needed to fill half of binding sites, i.e.,  $X_{g1} < X_{g2}$ , produces the condition  $X_h < 2(1 - e^{\Delta F})^{-2}$ ; in other words,  $X_g$  does not change with  $X_h$ . In this case, we have an excess of guest molecules over the binding sites and the boundary  $\phi_g = \phi_h$  is below the crossover  $\langle \theta \rangle = 1/2$  boundary.

On the other hand, if  $X_{g1} > X_{g2}$ , we have  $X_h > 2(1 - e^{\Delta F})^{-2}$ , and the  $\langle \theta \rangle = 1/2$  crossover is below the  $\phi_g = \phi_h$  line. Hence, if we increase the concentration of binding sites, we need more guest molecules to be able to fill half of the binding sites: their number grows as  $X_g = X_h/2e^{\Delta F}$ . Therefore, the existence of two regimes of low and high values of  $X_h$  is related to relative abundance of free guest monomers. For small number of bindings sites, the number

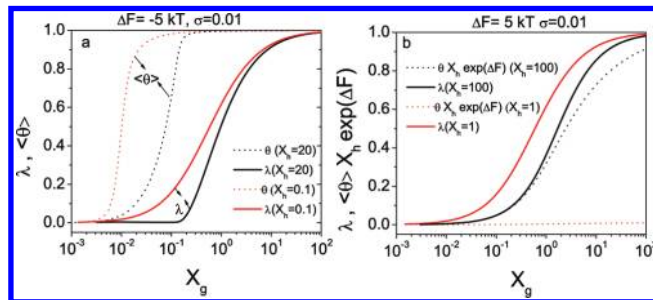


**Figure 3.** (a) Bound fraction  $\langle \theta \rangle$  (dotted lines) and fraction of self-assemblies of the guest molecules  $\lambda$  (solid lines) as a function of the mass action  $X_g$  for a template of length  $q = 10$ , degree of cooperativity  $\sigma = 0.01$ , and the energetic difference between the templated and nontemplated binding  $\Delta F = -5(k_B T)$  at two values of the mass action variable of host molecules  $X_h = 0.1$  and  $20$ . (b)  $\langle \theta \rangle X_h e^{\Delta F}$  (dotted lines) and fraction of self-assemblies  $\lambda$  (solid lines) as a function of  $X_g$  for a template of length  $q = 10$ ,  $\sigma = 0.01$ , and  $\Delta F = 5(k_B T)$  and at two different values of  $X_h = 1, 100$ .

of free monomers is much larger than what is needed to fill half of the template binding sites, while for large number of binding sites, almost all the monomers are consumed to fill half of templates, and the number of free monomers is negligible compared to the number of bound monomers.

To illustrate this, we plot in Figure 3a both  $\langle \theta \rangle$  and  $\lambda$  as a function of  $X_g$  for two different values of  $X_h$ , one much smaller and one much larger than  $2(1 - e^{\Delta F})^{-2} \approx 2$  for  $\Delta F \ll -1$ . It shows that for even when  $X_h \ll 2$  and the tendency to form host-guest complexes is small, almost all template sites are occupied even before  $\lambda$  approaches a value of one-half. For  $X_h \gg 2$  the fraction of guest molecules in self-assemblies remains practically zero before all the template sites are occupied, and only after that self-assemblies grow upon increasing the guest concentration,  $X_g$ , as is expressed in a growth of the quantity  $\lambda$ .

The existence of two regimes for the polymerization line  $\lambda = 1/2$  can be explained in a similar fashion, that is, in terms of the number of the available guest molecules. For small values of  $X_h$ , the number of monomers bound the templates is negligible in comparison to the number of monomers needed to have half of the guest material in the form of polymers; therefore,  $X_{gp}$ , defined as the guest mass action for which  $\lambda = 1/2$ , is the same as that of exclusive self-assembly, which happens for  $X_{gp} \approx 0.585$  (see ref 2). While for  $X_h > X_{gp} e^{-\Delta F}/2 \approx 43$  if  $\Delta F = -5$ , the sum of the concentration of monomers bound to the templates and of those in free solution is of the order of  $2X_h e^{\Delta F}$ . This concentration grows with increasing values of  $X_h$  and cannot be ignored; it plays an important role in position of the boundary of where self-polymerization takes off.

We now turn to the case  $\Delta F \geq 0$ , where the affinity of monomers toward each other is comparable to or stronger than their affinity toward the binding sites on the templates. In this situation, self-polymerization is the predominant state of the system, and the templates coverage never goes beyond  $\langle \theta \rangle (e^{-\Delta F}, \sigma)$ , which is practically zero for  $\Delta F = 5(k_B T)$ . Therefore, in this case there is practically no coexistence of templated and self-assembly. The asymmetry in the competition between templated and self-assembly for positive and negative values of  $\Delta F$  arises from the fact that there is no limit on self-polymerization as we increase the concentration of guest monomers, whereas for a given host concentration  $X_h$  the number of binding sites to be occupied by monomers remains constant. Note that if the strength of the binding to a template site and that attaching to a free end of a growing polymer are equal, implying that  $\Delta F = 0$ , the fraction of bound sites reaches at most a value of  $1/2$ , albeit only in the limits of very high guest concentrations infinitely long chains,  $q \rightarrow \infty$ .

Interestingly, we also observe two regimes for the polymerization line  $\lambda = 1/2$  if  $\Delta F > 0$ , starting off with an initially constant value of  $X_{gp} \approx 0.585$  for small  $X_h$ . The reason for the upturn for increasing values of  $X_h$  is the small but increasingly non-negligible number of monomers binding to the templates. The concentration of monomers bound to the templates and that of the free monomers times  $\exp(-\varepsilon_1)$  is proportional to  $2\langle\theta\rangle(e^{-\Delta F, \sigma})X_h e^{\Delta F}$ . This amount is indeed negligible for small values of  $X_h$  but does give rise to a considerable contribution for large  $X_h$ . It is for this reason that we observe a transition of the polymerization line from zero to a nonzero slope for  $X_h \approx X_{gp} e^{-\Delta F} / 2\langle\theta\rangle(e^{-\Delta F, \sigma})$ , which is approximately equal to 29 for the values  $\sigma = 0.01$  and  $\Delta F = 5(k_B T)$  used in Figure 2b. We can clarify the above by considering the quantities  $\langle\theta\rangle(e^{-\Delta F, \sigma})X_h e^{\Delta F}$  and  $\lambda$  as a function of  $X_g$ , which we have plotted in Figure 3b for two values of  $X_h$ , one being much smaller and one much larger than the transitional value  $X_h = 29$ . The figures show that for a small values of  $X_h$ ,  $\langle\theta\rangle(e^{-\Delta F, \sigma})X_h e^{\Delta F}$  is negligible for all the values of  $X_g$ , while for the larger value of  $X_h$ , this value grows with  $X_g$  and becomes comparable to  $X_{gp}$ .

In conclusion, in the templated-assembly dominant regime self-polymerization can only occur if the template sites are almost completely occupied. As a consequence, the presence of templates effectively suppresses self-polymerization of the guest molecules, unless a large excess of guest molecules is present in the solution and only then if the templates are already filled. So, before that this happens, self-assembly can be safely ignored. This special case has been discussed at length in the literature,<sup>24–28</sup> the most well-known of them being the seminal work of McGhee and von Hippel. Still, in spite of this a comprehensive discussion of the dependence of bound fraction on the template size, the cooperativity factor  $\sigma$  and the stoichiometric ratio as a function of the experimentally relevant tuning parameters remain lacking. We also note in passing that our Ising-like approach is more straightforward in comparison to earlier discussed probabilistic methods when it comes to extracting the explicit dependence of the bound fraction on various system parameters and obtaining a deeper understanding of templated assembly. Also, in a recent work modeling binding of small ionic molecules to polymers, an Ising-like approach has been employed,<sup>31</sup> however in that work, the binding statistics is considered at the mean-field level, while in our model the treatment of binding statistics is exact. Our next section is devoted to this issue.

#### 4. Exclusively Templated Assembly

As we discussed in the previous section, self-assembly does not interfere with templated assembly if  $\Delta F < 0$ . Formally, we can take the limit  $\varepsilon_1 \rightarrow \infty$  or  $\Delta F \rightarrow -\infty$  to study this case. In this situation,  $X_g \rightarrow 0$ , but this does not imply that the guest concentration  $\phi_g$  is zero. Therefore,  $X_g$  is no longer the relevant variable for a description of the system, and we instead replace it with the variable  $\eta \equiv \phi_g/\phi_h$ . This quantity is known as the stoichiometric ratio, and the pertinent set of variables for the description of our system is now given by  $X_h$ ,  $\eta$ , and  $\sigma$ . In the limit of  $\Delta F \rightarrow -\infty$ , the mass conservation equation, eq 10, reduces to

$$s = X_h(\eta - \langle\theta\rangle) \quad (12)$$

In the following, we give an extensive analysis of the model in order to understand how stoichiometry, template length, and cooperativity influence the fraction of occupied binding sites on the host template molecules  $\langle\theta\rangle$ . To this end, we investigate the functional dependence of  $\langle\theta\rangle$  on the mass action variable  $X_h$  for different values of the various parameters. We remind the reader that  $X_h \equiv \phi_h \exp(-\varepsilon_2 - g)$  measures the strength of the driving force toward host–guest binding and incorporates the dependence both on the concentration of host templates and on the stacking and binding free energies.

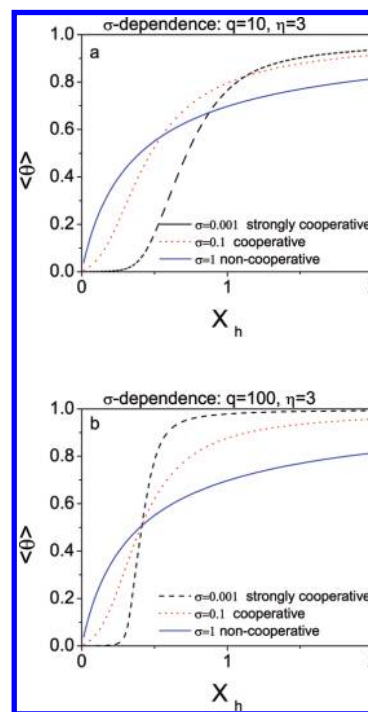


**Figure 4.** Bound fraction  $\langle\theta\rangle$  as a function of mass action variable  $X_h$  (see the text and list of symbols for explanations) for different values of cooperativity  $\sigma = 0.001, 0.1$ , and  $1$  (see the legends) on the templates of  $q$  sites at the stoichiometric ratio  $\eta = 3$ . The template lengths shown in panels a and b are  $q = 10$  and  $q = 100$ .

Looking at how  $\langle\theta\rangle$  varies with  $X_h$  for arbitrary values of the parameters  $\eta$ ,  $q$ , and  $\sigma$  in the model, we observe a general trend: a transition from empty, nonpolymerized templates with  $\langle\theta\rangle = 0$  for  $X_h = 0$  to some saturation value  $\langle\theta\rangle = \langle\theta\rangle_{max}$  that may be smaller than unity for large values of  $X_h$ . This transition is generally not sharp albeit that it varies with the values of any of the three pertinent system parameters  $\eta$ ,  $q$ , and  $\sigma$ . We investigate the role of each of these parameters explicitly, fixing the values of the other parameters.

For definiteness, we define as the “adsorption transition” that value of  $X_h$  at which half of the binding sites are occupied by guest molecules. According to this definition, we have  $\langle\theta\rangle = 1/2$  exactly at the adsorption transition  $X_{hp}$ . Its value depends on the template size  $q$ , the level of binding cooperativity  $\sigma$ , and the stoichiometric ratio  $\eta$ . However, for excess amounts of guest molecules  $\eta > 1$  and in the limit of long chains  $q \gg 1$ , it approaches the value  $1/(\eta - 1/2)$ . Furthermore, the sharpness of the transition can be defined as  $\partial\langle\theta\rangle/\partial X_h|_{X_{hp}}$ . We find it to be equal to  $(\eta - 1/2)/\sqrt{\sigma}$  in the infinite chain limit,  $q \rightarrow \infty$ . This already tells us that if  $\sigma \rightarrow 0$ , corresponding to a high degree of cooperativity, we get a true phase transition because the slope goes to infinity. The heat capacity in that case makes a jump at the transition temperature. To understand better how the level of cooperativity affects the sharpness of transition, we start with investigating the role of the parameter  $\sigma$  first.

**4.1. The Role of Cooperativity.** The level of cooperativity in the binding of the guest molecules to the host template is regulated by the parameter  $\sigma$ . It measures the influence of an already bound guest molecule on the binding of a new guest molecule adjacent to it. Not surprisingly, it is directly related to the interaction free energy of neighboring bound guest molecules  $\varepsilon_2$ , with  $\sigma \equiv \exp(\varepsilon_2)$ . Therefore, by varying the numerical value of  $\sigma$ , we alter the level of cooperativity in our system, which directly influences the sharpness of transition: the smaller  $\sigma$ , the higher level of cooperativity.

Figure 4 presents the bound fraction of sites as a function of mass action  $X_h$  for two different template sizes,  $q = 10$  and

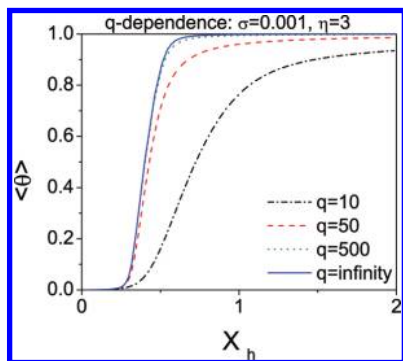


**Figure 5.** Bound fraction  $\langle\theta\rangle$  as a function of host mass action variable  $X_h$  for different template lengths  $q = 10, 50,$  and  $500$ , stoichiometric ratio  $\eta = 3$  and cooperativity parameter  $\sigma = 0.001$  giving rise to a correlation length of  $\xi_0(\sigma) \approx 16$ . The solid line shows the limit of curves for  $q \rightarrow \infty$ ; see eq 14 for further explanation.

100. From this figure, we conclude that irrespective of the size of the template, the smaller the value of  $\sigma$ , corresponding to larger values of stacking energy, the sharper the transition is. Note that  $\sigma = 1$  corresponds to noncooperative case, and as can be seen from the figure, in this case the sharpness of transition is considerably lower than that of the cooperative one.

An interesting case to consider is strong binding limit, i.e., when  $\varepsilon_2 \rightarrow -\infty$  for large  $q$ , corresponding to  $\sigma \rightarrow 0$ . In this limit, the asymptotic behavior of  $\langle\theta\rangle(X_h, q, \sigma)$  is of the form

$$\langle\theta\rangle = \frac{\sigma X_h \eta}{(1 - X_h \eta)^2} \quad X_h \ll X_{hp} = \frac{1 + 2/q}{\eta - 1/2} \quad (13)$$

$$\langle\theta\rangle = 1 - \frac{2}{q} \frac{1}{(X_h(\eta - 1) - 1)} \quad X_h \gg X_{hp}$$

Also, we can calculate the slope of  $\langle\theta\rangle$  at the transition point in this limit, giving  $\partial\langle\theta\rangle/\partial X_h|_{X_h \rightarrow X_{hp}} \approx q\sigma X_h(\eta - 1/2)/(1 - X_h(\eta - 1/2))^2$ . Setting  $q \rightarrow \infty$ ,  $\langle\theta\rangle$  approaches a Heaviside step function of the form  $H(X - X_{hp})$ . Therefore, this jump in the bound fraction occurring at  $X_{hp}$  is equivalent to the magnetization jump in the one-dimensional Ising model in zero-temperature limit.

Although increasing the cooperativity level for both  $q$  values plotted in Figure 4 raises the sharpness of transition, having a closer look at this figure, we find that for the same value of  $\sigma$  the transition is sharper the larger the template length  $q$ . Therefore, we explore in more detail the role of template size in the next subsection.

**4.2. Finite-Size Effects.** To investigate the dependence of the bound fraction on the length of the template, we have plotted in Figure 5  $\langle\theta\rangle$  as a function of  $X_h$  for different  $q$  values but fixed stoichiometry  $\eta = 3$  and level of cooperativity  $\sigma = 0.001$ . This figure clearly shows that as the templates become longer, the sharpness of transition increases so that for large enough  $q$  values the curves approach the infinite-chain limit shown by the solid line in the figure. This suggests that for template lengths larger than a characteristic length scale the behavior of system becomes weakly dependent on  $q$ . We expect that this length scale to be related to average length of segments of occupied sites on the template, characterizing the mean size of cooperative domains along the templates. Indeed, this reminds us of the correlation length, which in our case specifies the mean distance from an occupied (or empty) site beyond which there is a zero probability of having a bound (or empty) site.

In our model, the correlation length  $\xi$  is a decay length of the two-point correlation function of the occupation number.

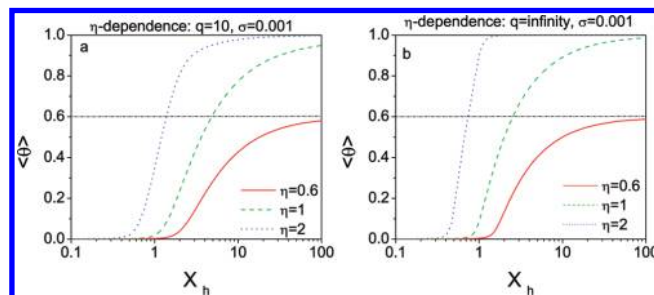


**Figure 6.** Bound fraction as a function of mass action  $X_h = \phi_h \exp(-\varepsilon_2 - g)$  for (a) a short template ( $q = 10$ ) and (b) a long template ( $q \rightarrow \infty$ ) at different values of stoichiometric ratio. The corresponding stoichiometric ratios of  $\eta = 0.6, 1,$  and  $2$  are shown in the legend. For all the curves  $\sigma = 0.001$ .

In the large- $q$  limit the correlation length can be expressed in terms of the two eigenvalues as  $\xi = 1/\ln(\lambda_1/\lambda_2)$ , which takes a simple form in the limit of strong cooperativity:  $\xi_0 \equiv \xi(s = 1, \sigma \ll 1, q \rightarrow \infty) \approx \sigma^{-1/2}/2$ .<sup>22</sup> For the typical value  $\sigma = 0.001$  used in Figure 5,  $\xi_0(\sigma) \approx 16$ . Thus, for  $q$  values considerably larger than  $\xi_0$ , the bound fraction approaches that of infinite-chain limit the corrections to it are on the order of  $1/q$ . As a result, for template sizes much larger than the correlation length we can use the infinite-chain limit approximation, which leads to a simple expression readily applicable for a quick fitting of experimental data

$$\langle\theta\rangle(s, \sigma) = \frac{1}{2} + \frac{1}{2} \frac{s - 1}{\sqrt{(1 - s)^2 + 4\sigma s}} \quad (14)$$

where the quantity  $s$  follows self-consistently from eq 15. These equations can be used to obtain the solid curve plotted in Figure 5.

Having a clear view of how cooperativity and template size influence the bound fraction, we now investigate how the relative abundance of guests and host binding sites (the stoichiometry) influences the binding efficiency.

**4.3. The Role of Stoichiometry.** The stoichiometric ratio  $\eta = \phi_g/\phi_h$  is defined as the ratio of mole fraction of guest molecules,  $\phi_g$ , to that of host binding sites,  $\phi_h$ . Obviously, in order to fill all the template sites, the number of guests must at least be equal to the number of binding sites, i.e.,  $\eta = 1$ . However, because of thermal fluctuations not all the guests will bind to the templates sites, and there are always some free guest molecules available in the solution, except for very high mass action values  $X_h \gg 1$  where all the guests are adsorbed on the templates. Thus, an excess of guest molecules over binding sites is necessary but not sufficient to fill all the binding sites.

To understand the influence of the stoichiometric ratio on the bound fraction better, we have plotted  $\langle\theta\rangle$  in Figure 6 as a function of mass action variable  $X_h$  for different values of  $\eta$  corresponding to three different cases  $\eta < 1$ ,  $\eta = 1$ , and  $\eta > 1$  for a short template and for an infinitely long chain. The cooperativity parameter for all the curves is the same  $\sigma = 0.001$ , i.e., a strong degree of cooperativity that enhances the efficiency of binding. We observe the general trend that  $\langle\theta\rangle$  increases gradually from zero to a saturation value  $\langle\theta\rangle_{max} \leq 1$  upon increasing the value of mass action variable  $X_h$ . The sharpness of the transition, as well as the saturation level  $\langle\theta\rangle_{max}$ , is influenced by the stoichiometric ratio  $\eta$ . As expected, when  $\eta < 1$ , the guest monomers cannot fill all the binding sites, and at most only a fraction of binding sites equal to  $\eta$  will be bound, i.e.,  $\langle\theta\rangle_{max} = \eta$ . For  $\eta \geq 1$ ,  $\langle\theta\rangle_{max} = 1$ ; one can reach the value 1 only for large enough  $X_h$ .

Especially, for  $\eta = 1$ , full saturation requires quite large values of  $X_h$ . Indeed, for  $\eta > 1$ , the larger the  $\eta$  value, the crossover from empty to full templates occurs at a lower value of the mass action variable  $X_h$  and the sharpness of transition as measured by the quantity  $\partial\langle\theta\rangle/\partial X_h|_{x_{hp}}$  increases.

In summary, a stoichiometric ratio larger than one enhances the binding efficiency, and to achieve full binding at not very large values of mass action variable  $X_h$ , an excess of guest molecules is required. On the other hand, for a stoichiometric ratio smaller than unity, not all the binding sites can be filled and the bound fraction saturates at a value equal to the stoichiometry ratio for large values of host mass action. This leads us to the issue of how precisely the guests are distributed over the templates for partially filled template sites. This is the subject of the next section.

### 5. Distribution Function of Occupied Sites

As already mentioned, the bound fraction, i.e., the mean filling fraction  $\langle\theta\rangle$ , is a quantity that can be probed experimentally. The product  $q\langle\theta\rangle$  then provides us with information about the average number of occupied sites per template. An interesting question that also arises is how, given this mean value, the filling fraction varies from one template to another. In other words, the question arises what the distribution of the filling fractions  $\theta = n/q$  is over the templates, where  $n$  is the number of occupied sites of a template, for a known value of  $0 < \langle\theta\rangle < 1$ . Of particular interest is whether or not a fraction  $\langle\theta\rangle\phi_h/q$  of templates is completely filled and the remainder is empty or that all the templates have the average  $q\langle\theta\rangle$  number of sites occupied. To answer this question, we need to find the probability distribution function  $P_q(\theta)$  of the filling fraction, which is defined as the normalized distribution of templates with  $n = q\theta$  occupied sites,  $\rho_i(n)$ , i.e.,  $P_q(\theta) = \rho_i(q\theta)q\nu/\phi_h$ .

As we discussed in section 2, the optimal distribution  $\rho_i(n)$  minimizes the grand potential. The grand potential is characterized by two main ingredients: a combinatorial factor counting the number of possible configurations leading to the same number of occupied sites and the Boltzmann weight associated with those configurations. The combinatorial factor is largest when the fragmentation of bound domains is largest (producing maximal entropy) while the Boltzmann factor favors minimizing the number of distinct domains (minimizing the interaction free energy between the bound guest molecules). Clearly, these two factors compete with each other in determining the most probable of configurations. As it turns out, the interplay between them is highly dependent on the length of templates.

For very short chains there is less combinatorial entropy available, simply because there is not enough room to move the domains about. As a result, states of either totally filled or empty templates are in that case preferred. In the other extreme of long chains, the combinatorial factor can benefit from large number of fragmentations, leading to many bound domains of moderate lengths of the order of correlation length. Therefore, we expect a crossover from an all or nothing distribution for short templates to a Gaussian distribution for long templates occurring at template lengths on the order of correlation length.

To obtain from eq 5, an explicit functional form for the probability distribution function of the filling fraction is not a trivial task. However, for the related problem of spins on a one-dimensional lattice, Shigematsu<sup>29</sup> has been able to calculate explicitly the normalized probability distribution function of the average spin state of the Ising chain, at least in the limit of large template lengths  $q \gg 1$  and strong coupling, so large values of  $|\varepsilon_2|$ , for a fixed and finite ratio of the chain length and the correlation length,  $q/\xi_0$ . We can exploit this result by a simple transformation of the average spin state of a single chain,  $\langle S \rangle = q^{-1} \sum_{i=1}^q S_i$ , to the filling fraction of our templates,  $\langle S \rangle = 2\theta - 1$ .

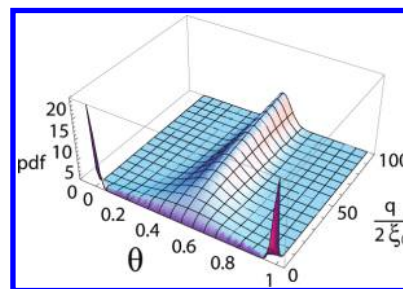


**Figure 7.** Probability distribution function (pdf) as a function of  $\theta$  and  $q/2\xi_0$  for the case  $\langle\theta\rangle = 1/2$ . The pdf becomes more and more centered around  $\theta = 1/2$ , as the length of templates is increased.

For large  $q$  values, the discrete rational values of  $\theta = n/q$  are replaced then by a continuous  $\theta$  variable varying between 0 and 1.

Implementing this mapping, we find that the probability distribution function (pdf) for the case of arbitrary  $\langle\theta\rangle$  consists of a discrete part, representing the all-or-nothing distribution, and a continuous part, representing the possibility of multiple fragmentations. The relative dominance of each contribution is determined by the ratio of chain length  $q$  and the correlation length  $\xi_0$  in the infinite chain limit. The complete form of the pdf for different values of  $0 < \langle\theta\rangle < 1$  can be found in the Supporting Information. Here, we present only the pdf formula for the case that  $\langle\theta\rangle = 1/2$ , corresponding to what we defined to be the polymerization point

$$P_\infty(\theta, x) = \frac{1}{2} e^{-x} [\delta(\theta - 1) + \delta(\theta) + x I_0(z) + x^2 z^{-1} e^{(2\theta - 1)y} I_1(z)] \quad (15)$$

where  $x \equiv q/2\xi_0$ ,  $z \equiv 2[\theta(1 - \theta)]^{1/2}$ , and  $\delta$  is defined as  $q$  times the Kronecker delta, that in the limit of  $q \rightarrow \infty$  becomes equivalent to a Dirac delta distribution. Finally,  $I_0$  and  $I_1$  are modified Bessel functions,  $I_n$ , of the first kind for the integer values  $n$  equal to 0 and 1.

The expression clearly shows that the probability distribution function of the number of occupied sites must exhibit a crossover between two distinct regimes characterized by large and small values of the quantity  $x = q/2\xi_0$ , as in fact expected from our earlier arguments. Integrating over the discrete and continuous part of the distribution function in eq 15, we find that contribution of these two parts becomes equal to each other if  $q/\xi_0 \approx 1.4$ . The pdf then crosses over from a fully discrete measure to a fully continuous measure. In Figure 7, we have plotted the pdf as a function of  $\theta$  and  $q/2\xi_0$ . To visualize the discrete part, we have approximated the delta functions with normalized Gaussians of a very small width (0.01). This figure indeed shows that the pdf becomes more peaked around the center  $\theta = 1/2$  as the  $q/2\xi_0$  increases and the contribution of the continuous part to the total pdf becomes dominant.

To get a better grasp of the influence of the template length on the distribution function, we find the limiting behavior of the pdf from eq 15 for two limits of  $x \ll 1$  and  $x \gg 1$

$$P_\infty(\theta; x \ll 1) = \frac{1}{2} [\delta(\theta - 1) + \delta(\theta)]$$

$$P_\infty(\theta; x \gg 1) = \left(\frac{x}{2\pi}\right)^{1/2} [4\theta(1 - \theta)]^{-1/4} [1 + [4\theta(1 - \theta)]^{-1/2}] \exp\left[2x\left(\sqrt{\theta(1 - \theta)} - \frac{1}{2}\right)\right] \quad (16)$$

In the limit of  $x \ll 1$ , short templates, the discrete part is fully dominant and the pdf is described by a discrete measure concentrated on the numbers 0, 1. This implies that short templates in the solution are either filled or empty. Mixed forms are not

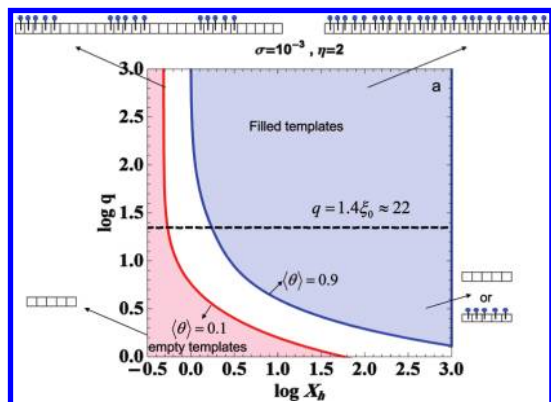


**Figure 8.** Configuration-state diagram as a function of the template length  $q$  and the mass-action variable  $X_h$ . Shown are results calculated for a stoichiometric ratio  $\eta = 2$ , degree of cooperativity  $\sigma = 10^{-3}$ , and  $\Delta F \rightarrow -\infty$ . The two contours of constant bound fraction of sites  $\langle \theta \rangle = 0.1$  and  $0.9$  are the boundaries of the transition region from sparsely to densely occupied host molecules. It should be noted that the width of the transition region varies as the template length  $q$  changes. For very long templates  $q \gg \xi_0$  the width is proportional to  $\sigma^{1/2}$ ; for short templates  $q \ll \xi_0$  the width is proportional to  $\sigma^{-1/q}$ . The horizontal dashed line at  $q = 1.4\xi_0$  shows the crossover from an all-or-nothing distribution for short templates to a continuous Gaussian-like distribution for long templates. See also Figure 7.

avored because of a lack of combinatorial entropy. In that case there are fewer mutually distinguishable distributions of bound guest molecules on the template. On the other hand, in the limit of  $x \gg 1$ , the continuous part is fully dominant, and one gets an almost Gaussian distribution with an expectation value  $\langle \theta \rangle = 1/2$  and width of  $1/2\sqrt{x}$  and the templates have alternating filled and empty sections with average lengths of the order  $\xi_0$ . In this case the combinatorial factor can benefit from a large number of entropically favorable fragmentation on a long chain.

Finally, we summarize the dominant configurations of templates from the perspective of the distribution of guests over them in state diagram in Figure 8. In this figure, the dominant bound states are shown as we vary the length of templates and the strength of host mass action variable  $X_h$ , for a set of values of  $\sigma$  and  $\eta$  in the limit of  $\Delta F \rightarrow -\infty$ . We can recognize three regions in the state diagram: (i) a region of virtually empty templates with  $\langle \theta \rangle < 0.1$ , (ii) a region of essentially fully covered templates with  $\langle \theta \rangle > 0.9$ , and (iii) a transition region, where  $0.1 < \langle \theta \rangle < 0.9$  and the templates are partially filled. The interesting region to discuss here is the transition region. In this region, for a known value of the bound fraction the distribution function of guests over the templates is very much dependent on the length of templates. Two distinct regimes can be seen as shown schematically in the figure based on our earlier discussion: an all-or-nothing distribution for template lengths short compared to the correlation length  $\xi_0$  and a continuous Gaussian-like distribution for very long templates compared to  $\xi_0$ . The width of transition region varies with degree of cooperativity as  $\sigma^{1/2}$  for long templates and  $\sigma^{-1/q}$  for short templates. We expect that the transition region width to depend on  $\Delta F$  as well. To investigate this, we have plotted in Figure 9 the boundary lines  $\langle \theta \rangle = 0.1$  and  $\langle \theta \rangle = 0.9$  for different values of  $\Delta F$ . We find that the boundary line  $\langle \theta \rangle = 0.1$  does not vary with  $\Delta F$  in the range investigated, while the boundary line  $\langle \theta \rangle = 0.9$  is highly dependent on  $\Delta F$ . This line shifts toward larger and larger host mass action variable as  $\Delta F$  becomes less negative and the competition between binding of a monomer on a template site adjacent to a bound site and to a self-polymer gets closer. Finally, it is worth mentioning that our state diagram of dominant configurations is, perhaps not entirely surprisingly, very similar to that of Zimm–Bragg for helix–coil transition of biopolymers.<sup>23</sup>

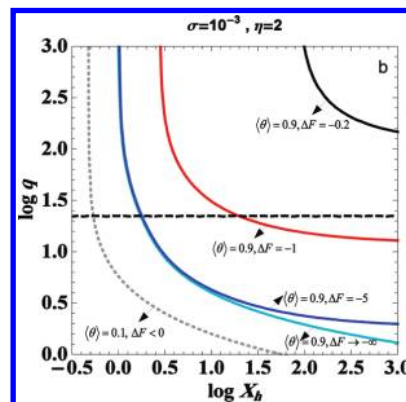


**Figure 9.** Configuration-state diagram as a function of the template length  $q$  and the mass-action variable  $X_h$ . Shown are results calculated for a stoichiometric ratio  $\eta = 2$  and degree of cooperativity  $\sigma = 10^{-3}$ . In addition to  $\langle \theta \rangle = 0.1$  and  $0.9$  in the limit  $\Delta F \rightarrow -\infty$ , the contour line  $\langle \theta \rangle = 0.9$  is shown for different values of  $\Delta F = -5, -1$ , and  $-0.2$ . The less negative  $\Delta F$  becomes, the more the boundary shifts toward larger values of  $X_h$ . As in Figure 8, the horizontal dashed line at  $q = 1.4\xi_0$  shows the crossover from an all-or-nothing distribution to a continuous Gaussian-like distribution for long template. See also Figure 7.

## 6. Link to Experiments

In the previous sections, we discussed how the bound fraction of host sites varies with the host mass action variable for varying control parameters such as the stacking free energy, the stoichiometric ratio, and so on. However, in experimental reality the bound fraction, or rather a quantity that can be related to it, is measured by means of, e.g., UV absorption or circular dichroism, not as a function of the mass action variable but rather the temperature. In order to make a direct link to experiments, we make explicit in this section the temperature dependence of the bound fraction of sites,  $\langle \theta \rangle$ , as well as the fraction of self-assemblies,  $\lambda$ .

Of course, the temperature dependence of  $\langle \theta \rangle$  and  $\lambda$  is implicit through the temperature dependence of the free energies  $\varepsilon_1(T)$ ,  $g(T)$ , and  $\varepsilon_2(T)$ . In the first approximation, one can always use a Taylor expansion for each of the free energies around some reference temperature  $T_p$ , leading to  $\varepsilon_i(T) \approx \varepsilon_i(T_p) - (T - T_p) \Delta H_{\varepsilon_i}(T_p)/T_p + \dots$  for  $(i = 1, 2)$  and to  $g(T) \approx g(T_p) - (T - T_p) \Delta H_g(T_p)/T_p + \dots$ , in which  $\Delta H_g(T_p)$  and  $\Delta H_{\varepsilon_i}(T_p)$  are the dimensionless enthalpy changes associated with binding and stacking of guest monomers at the reference temperature  $T_p$  (in units of  $k_B T_p$ ). The temperature  $T_p$  is arbitrary, but we choose it as the point for which  $\langle \theta \rangle(T_p) = 1/2$ , i.e., when half the binding sites are occupied.

For our purposes, it turns out more practical to use one mass action variable  $X_h$ , one stoichiometric ratio  $\eta$ , and the two free energies  $\sigma$  and  $\Delta F$  as the independent set of variables. In this representation, the mass conservation equation eq 10 can be rewritten as

$$\frac{s}{(1 - se^{\Delta F})^2} + X_h[\langle \theta \rangle(s, \sigma, q) - \eta] = 0 \quad (17)$$

The temperature dependence of the host mass action variable  $X_h$  and cooperativity parameter  $\sigma$  are then  $X_h(T) = X_h(T_p) \exp[\Delta h(T_p)(T - T_p)/T_p]$ , with  $\Delta h(T_p) = \Delta H_g(T_p) + \Delta H_2(T_p)$  an effective binding enthalpy to a template site and  $\sigma(T) = \sigma(T_p) \exp[-\Delta H_{\varepsilon_2}(T_p)(T - T_p)/T_p]$ . Incorporating the temperature dependence of these free energies in eq 17, we can obtain  $T$  as a function of the quantity  $s$  that we from now on treat as a dummy variable. Therefore, solving the equations for the bound fraction  $\langle \theta(s) \rangle$  and the temperature  $T(s)$  self-consistently, we obtain the explicit temperature dependence of the bound fraction.

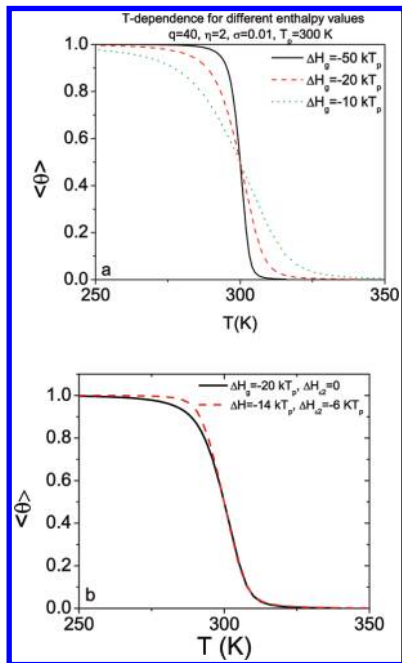


**Figure 10.** Bound fraction  $\langle\theta\rangle$  as a function the temperature  $T$ , for a stoichiometric ratio of  $\eta = 2$ , cooperativity factor  $\sigma(T_p) = 0.01$ , and template length  $q = 40$ . (a) Results for different values of enthalpy change  $\Delta H_g(T_p)$  and fixed  $\Delta H_{\varepsilon_s} = 0$  as shown in the legend. (b) Total enthalpy change of  $\Delta h(T_p) = 20k_B T_p$  for two cases: (i)  $\Delta H_{\varepsilon_s}(T_p) = 0$  and  $\sigma(T) = \sigma(T_p) = \text{constant}$  and (ii)  $\Delta H_{\varepsilon_s}(T_p) = -6k_B T_p$ , the latter leading to a temperature-dependent  $\sigma$ . We have assumed a polymerization temperature of  $T_p = 300\text{ K}$  for all the curves.

As we discussed in section 3, in the templated-assembly dominant state,  $\Delta F < 0$ , the templated assembly does not interfere with the self-assembly until all the templates are filled. This means that bound fraction as a function of temperature behaves the same as the case  $\Delta F \rightarrow -\infty$ . Taking this limit simplifies extracting the temperature from eq 17, as  $\Delta H_{\varepsilon_s}(T_p)$  drops out of this equation. Therefore, by fitting the temperature-dependent experimental data for  $\langle\theta\rangle$ , one can obtain values for both the total enthalpy change and cooperativity parameter.

To understand the influence of variations of each of the enthalpies in our model, we first consider the case that  $\Delta H_{\varepsilon_s}(T_p) = 0$ ; i.e., we suppress any temperature dependence of  $\sigma(T) \equiv \sigma(T_p)$ . The temperature  $T$  can be expressed to first order in  $T - T_p$  in terms of  $X_h$ , which in turn is expressed as a function of  $s$  from eq 12, i.e.,  $X_h = s/(\eta - \langle\theta\rangle)$ , and one can obtain the temperature dependence of the bound fraction  $\langle\theta\rangle$  from  $T(s)$  and  $\langle\theta\rangle(s)$  parametrized in terms of the dummy variable  $s$ . Results have been plotted in Figure 10a for the case of  $\Delta H_{\varepsilon_s} = 0$  and different values of enthalpy change  $\Delta H_g$  keeping all the other parameters fixed. These curves clearly demonstrate that the rate of saturation of the bound fraction of guest molecules,  $\langle\theta\rangle$ , upon cooling the system is strongly influenced by enthalpy change due to binding of guest molecules to the host molecules. In other words, the sharpness of the transition is controlled by  $\Delta H_g$ , the effective binding enthalpy to the host molecules.

In Figure 10b, we compare the temperature dependence of  $\langle\theta\rangle$  for two cases: (i)  $\Delta H_{\varepsilon_s} = 0$  and (ii)  $\Delta H_{\varepsilon_s} = -6k_B T_p$ , the latter value leading to a temperature-dependent cooperativity parameter  $\sigma$ . Both cases have the same value for total enthalpy change  $\Delta h = -20k_B T_p$ . As can be seen from this figure, the temperature dependence of  $\sigma$  shows its influence only at temperatures below  $T_p$  and leads to the saturation of the bound fraction at somewhat higher temperatures albeit that the effect is small. This figure suggests that the slope of  $\langle\theta\rangle$  around  $T = T_p$  is determined by the total enthalpy value  $\Delta h$ .

It is straightforward (if somewhat tedious) to show that at  $T = T_p$  the slope of  $\langle\theta\rangle$  at polymerization temperature  $T_p$ , for large enough  $q$  values  $q \gg \xi_0$  and  $\eta > 1$ , obeys

$$\left. \frac{d\langle\theta\rangle}{dT} \right|_{T=T_p} \approx \frac{\Delta h(T_p)}{T_p} \frac{\eta - 1/2}{1 + 4(\eta - 1/2)\sqrt{\sigma(T_p)}} \left[ 1 + \frac{4(\eta - 1/2)(\sqrt{\sigma(T_p)} - 1)}{1 + 4(\eta - 1/2)\sqrt{\sigma(T_p)}} \right] + O(q^{-2}) \quad (18)$$

This slope is sensitive to the dimensionless enthalpy  $\Delta h$  as well as the stoichiometric ratio  $\eta$  and the value of the cooperativity parameter at polymerization temperature  $\sigma(T_p)$ . In addition, it includes the correction of the order of  $1/q$  for large  $q \gg \xi_0$ . In the limiting case of infinite excess of guest molecules so that  $\eta(\sigma(T_p))^{1/2} \gg 1$ , this slope takes the simpler form of  $(\Delta h(T_p)/4T_p(\sigma(T_p))^{1/2})(1 - 1/(q(\sigma(T_p))^{1/2}))$ , which, interestingly, is independent of  $\eta$ . In the opposite limit of  $\eta(\sigma(T_p))^{1/2} \ll 1$ , the slope takes also a simple form  $\Delta h(T_p)(\eta - 1/2)/T_p$ , showing a linear dependence on stoichiometric ratio. The behavior of the slope on these two limits suggests that increasing  $\eta$  few times larger than one up to  $\eta(\sigma(T_p))^{1/2} \approx 1$  enhances the binding efficiency. However, exceeding this limit does not help the binding efficiency any further. This information can be used for a quick estimate of enthalpy values from the temperature-dependent data of bound fraction.

Another quick estimate of  $\Delta h(T_p)$  can be obtained from the dependence of polymerization temperature  $T_p$  on the size of template  $q$ . In the large  $q$  limit, the template size dependence of  $T_p$  can be obtained from the ratio of host mass action variable at  $T_p(q, \sigma)$  to its value at the polymerization temperature in the limit  $q \rightarrow \infty$ ,  $T_p(\infty)$ , and using eq 12, i.e.,  $X_h(T_p(q, \sigma))/X_h(T_p(\infty)) = s_p(q, \sigma)$ , which is independent of  $\eta$ . This leads to the following  $q$  dependence for  $T_p$

$$T_p(q, \sigma) \approx T_p(\infty) \left( 1 + \frac{2(1 - \sqrt{\sigma(T_p)})}{\Delta h(T_p(\infty))} \frac{1}{q} \right) + O\left(\frac{1}{q^2}\right) \quad (19)$$

up to  $1/q$  corrections. However, this expression becomes exact for the noncooperative case of  $\sigma = 1$ , and there is no correction due to finite length and for the cooperative case; the  $\sigma$  dependence is weak as also evidenced by Figure 10b. In the cooperative case, for a negative  $\Delta h$ , this tells us that the longer the template, the templated assembly saturates at a higher temperature.

At sufficiently low temperatures when the bound fraction has saturated, self-polymerization at some point sets in (unless  $\Delta F \rightarrow -\infty$ , of course). In such a situation, any UV absorbance or CD effect that probes interactions between (helically) stacked guest molecules is plausibly proportional to the overall fraction of polymers, i.e.,  $f = \langle\theta\rangle/\eta + \lambda$ , so consisting of contributions from material in templated and in self-assemblies. To investigate this, we calculated the temperature dependence of the bound fraction and the fraction of self-assemblies explicitly, using the full mass conservation equation eq 17 for a particular choice of parameters. In Figure 11, we have plotted both the bound fraction and the fraction of self-assemblies as well as the total fraction of polymers as a function of the temperature. The enthalpy values used here are comparable to what was extracted from experiments in refs 18 and 19.

This figure leads us to two important insights. First, the fraction of self-assemblies can indeed be ignored before  $\langle\theta\rangle$  saturates as in fact we already expected from our earlier discussion (see section 3). Second, the total fraction of polymers shows

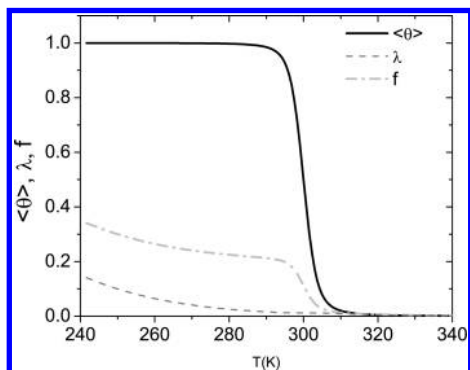


**Figure 11.** Bound fraction  $\langle\theta\rangle$  (solid line), fraction of self-assemblies  $\lambda$  (dashed line), and overall fraction of polymers,  $f = \theta/\eta + \lambda$ , as a function of the temperature for a template in the infinite-chain limit  $q \rightarrow \infty$ , with the interaction parameters values  $\Delta F(T_p) = -5kT_p$ ,  $\sigma = 0.01$ ,  $\eta = 5$ , and  $T_p = 300$  K. The enthalpy values used here are  $\Delta H_g(T_p) = -20kT_p$ ,  $\Delta H_{\varepsilon_1}(T_p) = -15kT_p$ , and  $\Delta H_{\varepsilon_2}(T_p) = -5kT_p$ . Notice that self-assembly does not occur appreciably until all the templates sites are filled.

an upward trend with decreasing temperature after all the templates are filled due to the start of self-polymerization. Such a temperature dependence has indeed been observed in UV-absorption experiments by Janssen and collaborators.<sup>19</sup> Hence, our theory provides a plausible explanation for the nonsaturating temperature dependence observed at low temperatures, although it could also originate from other effects, such as optical or change in supramolecular structure at lower temperatures. In our view, clarifying this issue merits further experimental studies.

## 7. Concluding Remarks

To describe competition of templated- and self-assembly, we present a coarse-grained model that is a combination of theory of linear self-assembly and an Ising-like model for templated assembly. The model that we advance hinges on three free energies associated with the binding free energy of a monomer on an empty site in a template,  $g$ , the stacking interaction of two monomers in a supramolecular polymer,  $\varepsilon_1$ , and that of two adjacent bound monomers on the template,  $\varepsilon_2$ . The crucial parameter determining the predominant state of assembly is a combination of these three free energies  $\Delta F \equiv g + \varepsilon_2 - \varepsilon_1$ , in essence the difference in free energy gain of a monomer attached adjacent to a bound site on the template and that of binding a monomer to a supramolecular polymer.

If  $\Delta F \geq 0$ , monomers tend to self-assemble rather than to bind to the templates, and self-polymerization is the predominant state. In this case, the average fraction of bound guest molecules to the templates can never reach the value of one-half, as there is no limit on the number of monomers that can self-assemble. For  $\Delta F < 0$ , the monomers have a stronger affinity toward templates than to each other. Upon increasing the monomer concentration for a fixed concentration of host templates large enough so that  $X_h > 2/(1 - e^{\Delta F})^2$ , first virtually all the binding sites are filled and only after the complexation saturates self-polymerization takes off. This brings us to the important conclusion that in templated-assembly dominant regime, the templated- and self-assembly do not interfere before virtually all of the binding sites are occupied by bound guest molecules. Hence, for all intents and purposes, one can treat the complexation problem in terms of the dependence of the bound fraction on various control parameters such as stoichiometric ratio, temperature, etc., as if there were exclusively templated assembly and self-assembly were somehow suppressed.

We find that the binding efficiency of templated assembly increases dramatically with increasing the stacking interaction, in

the sense that it raises the level of binding cooperativity leading to a much sharper transition from empty to filled templates. Interestingly, we also find that the length of the template has a similar influence and that the longer the template, the sharper the transition is albeit that the effect does saturate for chains much larger than the correlation length of the bound guest molecules. We come back to this below.

Another important determining factor for the sharpness of the transition is the stoichiometric ratio. It is often assumed in experimental studies that a 1:1 ratio of guest to host binding sites is optimal for effective filling of all the binding sites of the templates. However, as our model shows, at a stoichiometric ratio of one thermal fluctuations prevent the templates to all get filled except at very low temperatures, and the transition is definitely not sharp even at high degrees of cooperativity. Increasing the relative abundance of guests to a few times the number of binding sites enhances the efficiency of binding to templates dramatically and allows for effective filling of templates within limited range of temperature.

Our model can be used to fit to experimental data and extract the enthalpy values associated with the binding and stacking free energies as well as the cooperativity parameter. Indeed, we successfully fitted the data of Janssen et al.<sup>19</sup> on mixtures of oligo-thymine templates and naphthalene-like guest molecules, even though we ignored the possibility of competing self-assembly that indeed does seem to set in at low temperatures. It is clear now why this is so: the binding strength is strong enough to suppress it until all the templates are more or less filled. In relation to the experimental situation, if we assume that in a first order approximation  $\varepsilon_1 \approx \varepsilon_2$ , then  $\Delta F \approx g < 0$ . This suggests that as long as  $g$  is large enough, the templated assembly is dominant and the case  $\Delta F > 0$  is improbable in practical situations.

We emphasize that although models for the description of purely templated assembly have been developed long before,<sup>24</sup> their full theoretical characterization has so far been lacking. Here, we have filled in this gap and provided such a detailed analysis. Specifically, we have discussed how the guest monomers distribute themselves over the templates for the case of incomplete filling of the templates. From the insight obtained from our Ising-like model, we now understand that depending on the length of templates relative to the aforementioned correlation length that is set by the stacking free energy  $\varepsilon_2$ , different types of distribution are preferred. This correlation length is defined as the mean number of correlated template binding sites and is a measure of the average number of subsequent template sites in the infinite chain limit. For very short templates, i.e., shorter than the correlation length, the guests are distributed according to an all-or-nothing distribution, so a fraction of templates equal to the bound fraction are totally filled and the rest of them are empty. For very long templates, on the other hand, the guests are more or less evenly distributed over all the templates according to a Gaussian distribution centered around the average bound fraction.

A final issue worth mentioning here is the “squeezing out” of allowed template backbone configurations and a concomitant local stiffening of this backbone resulting from the binding of the guest monomers.<sup>30</sup> These effects are not taken into account explicitly in our quasi one-dimensional model. We argue that they are, however, described implicitly in the various effective free energy parameters. This is valid only in the limit where long-range self-interactions of the backbone is not important yet, that is, if the host molecules are not very long or if the solvent is near  $\theta$ -conditions. Clearly, this issue merits further study.

**Acknowledgment.** This work was part of the Research Programme of the Dutch Polymer Institute (DPI), Eindhoven, The Netherlands, as Project No. 610. We thank Pim Janssen, Albert Schenning, and Bert Meijer for stimulating discussions.

**Supporting Information Available:** Probability distribution function. This material is available free of charge via the Internet at <http://pubs.acs.org>.

### List of Symbols

$\varepsilon_1$	free energy of the bonded interaction between two monomers in a self-assembly, in units of the thermal energy $k_B T$
$\varepsilon_n$	nucleation free energy in units of $k_B T$
$\varepsilon_2$	stacking free energy in units of $k_B T$ between two adjacent monomers bound to the same template
$\sigma = \exp(\varepsilon_2)$	degree of cooperativity of binding guest on host molecules
$g$	free energy of binding of a monomer to a binding site on the template in units of $k_B T$
$\Delta F \equiv \varepsilon_2 + g - \varepsilon_1$	free energy difference of attaching a guest to a template next to an occupied site and that of attaching one to a free end of a self-assembled linear polymer
$s \equiv \exp(-\varepsilon_2 - g + \mu)$	measure of the strength of guest binding to the host
$\rho_g(N)$	the number density of chains of degree of polymerization $N$
$\rho_h(n)$	the number density of templates with $n$ bound monomers
$\mu_g$	chemical potential of guest molecules
$\mu_h$	chemical potential of host molecules
$\phi_g$	molar fraction of guest molecules
$\phi_h$	molar fraction of host molecules
$\eta = \phi_g/\phi_h$	stoichiometric ratio
$q$	number of binding sites on a template molecule
$\theta = n/q$	fraction of occupied sites on a template of size $q$
$\langle \theta \rangle$	mean filling fraction
$\lambda$	mean fraction of self-assemblies
$X_g \equiv \phi_g \exp(-\varepsilon_1)$	guest mass action variable
$X_{gp}$	polymerization point of self-assembly
$X_h \equiv \phi_h \exp(-\varepsilon_2 - g)$	host mass action variable
$X_{hp}$	polymerization point of templated assembly
$T_p$	polymerization temperature
$\xi_0$	correlation length in the limit of high cooperativity $\sigma \ll 1$
$x = q/2\xi_0$	ratio of template size and correlation length
$P_\infty(\theta, x)$	probability distribution function as a function of filling fraction and ratio of template size to correlation length for a known value of bound fraction

$\Delta H \varepsilon_i$	enthalpy change associated with binding free energy $\varepsilon_i$
$\Delta H_g$	enthalpy change associated with binding free energy $g$
$\Delta h \equiv \Delta H_{\varepsilon_2} + \Delta H_g$	relevant enthalpy for binding to a template

### References and Notes

- (1) Ariga, K.; Hill, J. P.; Lee, M. V.; Vinu, A.; Charvet, A.; Acharya, S. *Sci. Technol. Adv. Mater.* **2008**, *9*, 014109.
- (2) *Supramolecular Polymers*, 2nd ed.; Ciferri, A., Ed.; CRC Press: Boca Raton, FL, 2005.
- (3) Rothmund, P. W. K. *Nature* **2006**, *440*, 297–302.
- (4) Mao, C.; Sun, W.; Seeman, N. C. *Nature* **1997**, *386*, 137–138.
- (5) Martin, R. *Chem. Rev.* **1996**, *96*, 3043–3064.
- (6) Brunsfeld, L.; Folmer, B. J. B.; Meijer, E.; Sijbesma, R. P. *Chem. Rev.* **2001**, *101*, 4071–4097.
- (7) Zhao, D.; Moore, J. S. *Org. Biomol. Chem.* **2003**, *1*, 3471.
- (8) Bouteiller, L. *Adv. Polym. Sci.* **2007**, *207*, 79–112.
- (9) Klug, A. *Philos. Trans. R. Soc. London B* **1999**, *354*, 531–535.
- (10) Larson, S. B.; McPherson, A. *Curr. Opin. Struct. Biol.* **2001**, *11*, 59–65.
- (11) Xu, Y.; Ye, J.; Liu, H.; Cheng, E.; Yang, Y.; Wang, W.; Zhao, D.; Zhou, M.; Liu, D.; Fang, R. *Chem. Commun.* **2008**, 49–51.
- (12) Zlotnick, A. *Virology* **2003**, *315*, 269–274.
- (13) Abuladze, N. K.; Gingery, M.; Tsai, J.; Eiserling, F. A. *Virology* **1994**, *199*, 301–310.
- (14) Leger, J. F.; Robert, J.; Bourdieu, L.; Chatenay, D.; Marko, J. F. *Proc. Natl. Acad. Sci. U.S.A.* **1998**, *95*, 12295–12299.
- (15) Bull, S. R.; Palmer, N. J.; Liam, C.; Fry, Greenfield, M. A.; Messmore, B. W.; Meade, T. J.; Stupp, S. I. *J. Am. Chem. Soc.* **2008**, *130*, 2742–2743.
- (16) de la Escosura, A.; Verwegen, M.; Sikkema, F. D.; Comellas-Aragones, M.; Kirilyuk, A.; Rasing, T.; Nolte, R. J. M.; Cornelissen, J. J. L. M. *Chem. Commun.* **2008**, 1542–1544.
- (17) Xu, Y.; Ye, J.; Liu, H.; Cheng, E.; Yang, Y.; Wang, W.; Zhao, M.; Zhou, D.; Liu, D.; Fang, R. *Chem. Commun.* **2008**, 49–51.
- (18) Janssen, P. G. A.; Vandenbergh, J.; van Dongen, J. L. J.; Meijer, E. W.; Schenning, A. P. H. J. *J. Am. Chem. Soc.* **2007**, *129*, 6078–6079.
- (19) Janssen, P. G. A.; Jabbari-Farouji, S.; Surin, M.; Vila, X.; Gielen, J. C.; de Greef, T. F. A.; Vos, M. R. J.; Bomans, P. H. H.; Sommerdijk, N. A. J. M.; Christianen, P. C. M.; Leclere, P.; Lazzaroni, R.; van der Schoot, P.; Meijer, E. W.; Schenning, A. P. H. J. *J. Am. Chem. Soc.* **2009**, *131*, 1222–1231.
- (20) Dudowicz, J.; Douglas, J. F.; Freed, K. F. *J. Chem. Phys.* **2009**, *130*, 084903.
- (21) Bellot, M.; Bouteiller, L. *Langmuir* **2008**, *24*, 14176–14182.
- (22) Goldenfeld, N. *Lectures on Phase Transitions and Renormalization Group*, 1st ed.; Addison-Wesley Publishing Co.: Reading, MA, 1992.
- (23) Zimm, B. H.; Bragg, J. K. *J. Chem. Phys.* **1957**, *31*, 526–535.
- (24) McGhee, J. D.; von Hippel, P. H. *J. Mol. Biol.* **1974**, *86*, 469–489.
- (25) Epstein, I. R. *Biophys. Chem.* **1978**, *8*, 327–339.
- (26) Schwarz, G. *Biophys. Chem.* **1977**, *6*, 65–76.
- (27) Tsuchiya, T.; Szabo, A. *Biopolymers* **1982**, *21*, 979–994.
- (28) Di Cera, E.; Kong, Y. *Biophys. Chem.* **1996**, *61*, 107–124.
- (29) Shigematsu, H. *J. Stat. Phys.* **1990**, *71*, 981–1002.
- (30) Fredrickson, G. H. *Macromolecules* **1993**, *26*, 2825–2831.
- (31) Nakamura, S.; Shi, A.-C. *J. Chem. Phys.* **2010**, *132*, 194103.